Inorg. Chem. **2009**, *48*, 1168−1172

Synthesis of Urchin-like VO_2 Nanostructures Composed of Radially Aligned Nanobelts and Their Disassembly

Guicun Li,* Kun Chao, Chuanqin Zhang, Qingshan Zhang, Hongrui Peng, and Kezheng Chen

Key Laboratory of Nanostructured Materials, College of Materials Science and Engineering, Qingdao University of Science and Technology, Qingdao 266042, People's Republic of China

Received August 26, 2008

Urchin-like VO_2(B) nanostructures composed of radially aligned nanobelts have been synthesized by the homogeneous reduction reaction between peroxovanadic acid and oxalic acid under hydrothermal conditions. The influences of synthetic parameters, such as reaction times and the concentration of oxalic acid, on the morphologies and crystals of the resulting products have been investigated. The formation of VO_2(B) nanostructures undergoes a reduction-dehydration phase-transition and disassembly process. As the reaction time increases from 2 to 6 h, the diameters of urchin-like $V_{10}O_{24} \cdot 12H_2O$ nanostructures increase from 1−2 μm to 3−6 μm. After 12 h, urchin-like $V_{10}O_{24} \cdot 12H_2O$ nanostructures can be transformed in situ into VO_2(B) nanostructures composed of radially aligned nanobelts, which can be described by a possible reduction−dehydration phase-transition process. The urchin-like VO_2(B) nanostructures are disassembled into dissociated VO_2(B) nanobelts with the reaction time increased to 24 h. The shapes of the dissociated VO_2(B) nanobelts can be controlled by adjusting the concentration of oxalic acid.

Introduction

Bulk vanadium dioxide (VO_2) with a complex phase behavior dictated by strong electron−lattice correlations can undergo a Mott metal−insulator transition as well as a structural phase transition at around 67 °C, which is accompanied by abrupt changes in the optical and electrical properties of the oxide.[1−3] Recently, Qzailbash et al.[4] have reported a strongly correlated conducting state exists within the insulator-to-metal transition region in VO_2 in the form of nanoscale metallic puddles, and the electromagnetic response of these metallic puddles separated by the insulating host displays the signatures of collective effects in the electronic system including divergent optical effective mass and optical pseudogap.

In recent years, there has been intensive interest in low-dimensional (LD) VO_2 nanostructures including 0D, 1D, and 2D nanostructures because of their novel physical and chemical properties differing from their bulk counterparts.[5−10] For example, Lopez et al.[7,8] have observed that the optical contrast between the semiconducting and metallic phases of VO_2 nanoparticles is dramatically enhanced in the visible region, exhibiting size-dependent multipole optical resonance and transition temperatures. A variety of synthetic strategies such as vapor transport method,[11−13] sol−gel,[14−16]

* To whom correspondence should be addressed. Tel: 86-532-84022869. Fax: 86-532-84022869. E-mail: guicunli@qust.edu.cn.

(1) Morin, F. J. *Phys. Rev. Lett.* **1959**, *3*, 34.
(2) Biermann, S.; Poteryaev, A.; Lichtenstein, A. I.; Georges, A. *Phys. Rev. Lett.* **2005**, *94*, 026404.
(3) Kübler, C.; Ehrke, H.; Huber, R.; Lopez, R.; Halabica, A.; Haglund, R. F., Jr.; Leitenstorfer, A. *Phys. Rev. Lett.* **2007**, *99*, 116401.
(4) Qazilbash, M. M.; Brehm, M.; Chae, B. G.; Ho, P. C.; Andreev, G. O.; Kim, B. J.; Yun, S. J.; Balatasky, A. V.; Maple, M. B.; Keilmann, F.; Kim, H. T.; Basov, D. N. *Science* **2007**, *318*, 1750.
(5) Lopez, R.; Haglund, R. F., Jr.; Feldman, L. C.; Boatner, L. A.; Haynes, T. E. *Appl. Phys. Lett.* **2004**, *85*, 5191.
(6) Pietrzyk, P.; Sojka, Z.; Dzwigaj, S.; Che, M. *J. Am. Chem. Soc.* **2007**, *129*, 14174.
(7) Lopez, R.; Haynes, T. E.; Boatner, L. A.; Feldman, L. C.; Haglund, R. F., Jr. *Phys. Rev. B* **2002**, *65*, 224113.
(8) Lopez, R.; Feldman, L. C.; Haglund, R. F., Jr. *Phys. Rev. Lett.* **2004**, *93*, 177403.
(9) Park, J.; Oh, I. H.; Lee, E.; Lee, K. W.; Lee, C. E. *Appl. Phys. Lett.* **2007**, *91*, 153112.
(10) Gentle, A.; Maaroof, A. I.; Smith, G. B. *Nanotechnology* **2007**, *18*, 025202.
(11) Guiton, B. S.; Gu, Q.; Prieto, A. L.; Gudiksen, M. S.; Park, H. *J. Am. Chem. Soc.* **2005**, *127*, 498.
(12) Wu, J.; Gu, Q.; Guiton, B. S.; Leon, N. P.; Ouyang, L.; Park, H. *Nano Lett.* **2006**, *6*, 2313.
(13) Sohn, J. I.; Joo, H. J.; Porter, A. E.; Choi, C. J.; Kim, K.; Kang, D. J.; Welland, M. E. *Nano Lett.* **2007**, *7*, 1570.
(14) Mai, L. Q.; Hu, B.; Hu, T.; Gu, E. D. *J. Phys. Chem. B* **2006**, *110*, 19083.
(15) Chae, B. G.; Kim, H. T.; Yun, S. J.; Kim, B. J.; Lee, Y. W.; Youn, D. H.; Kang, K. Y. *Electrochem. Solid-State Lett.* **2006**, *9*, C12.
(16) Baudrin, E.; Sudant, G.; Larcher, D.; Dunn, B.; Tarascon, J. M. *Chem. Mater.* **2006**, *18*, 4369.

10.1021/ic801620n CCC: $40.75
Published on Web 01/06/2009

chemical vapor deposition,[17,18] pulsed laser ablation,[19] magnetron sputtering,[10,20] template-assisted synthesis,[21] thermolysis,[22] and solution-based synthesis,[23−29] have been developed to fabricate LD VO_2 nanostructures owing to their potential applications in lithium batteries,[16,26−28] intelligent window coatings,[17,18,20] Mott field-effect transistors,[11] and electrical-optical switching devices.[10,13] Among them, the solution-based method seems to be promising for the large-scale synthesis of VO_2 nanostructures because some rigid experimental conditions such as high temperature, and special equipments, are not necessary. In the solution-based synthesis, the formation of 1D VO_2 nanostructures including nanorods, nanowires, and nanobelts, is usually dependent on the types of reductants, such as formic acid,[23] oxalic acid,[24] ethylene glycol,[25] borohydride,[28] butanol,[29] and surfactants[27] because of the high redox-activity of vanadium oxide and their derivatives.[30−32] The dissolution of V_2O_5 in the H_2O_2 aqueous solution will result in peroxovanadic acid, which is an environmentally friendly precursor for V_2O_5 or V_2O_5 nanostructures.[32,33] The reduction of peroxovanadic acid inspires us to find a new route to VO_2 nanostructures. Herein, we report a facile approach for the synthesis of urchin-like VO_2(B) nanostructures composed of radially aligned nanobelts by a homogeneous reduction reaction between peroxovanadic acid and oxalic acid. A phase-transition process from monoclinic $V_{10}O_{24}\cdot 12H_2O$ to monoclinic VO_2(B) is observed for the first time during the reduction−dehydration process.

Experimental Section

Synthesis of VO_2(B) Nanostructures. Commercial orthorhombic V_2O_5 powders (0.36 g) were dissolved into 2 mL of 30% H_2O_2 solution, followed by the addition of 40 mL of distilled water with stirring to form an orange solution. Then, 40 mL of 0.1 mol/L oxalic acid (4 mmol) solution was added to the above solution. The mixed orange solution was placed in a 100 mL autoclave with a Teflon liner. The autoclave was maintained at 180 °C for different reaction times and then air cooled to room temperature. The resulting precipitates were collected and washed with distilled water several times and then dried in vacuum at 60 °C for 10 h. In all reactions, the content of commercial V_2O_5 powders is kept unchanged. As the reaction time increases from 0.5 to 12 h, the color of the resulting products changes from green to dark blue.

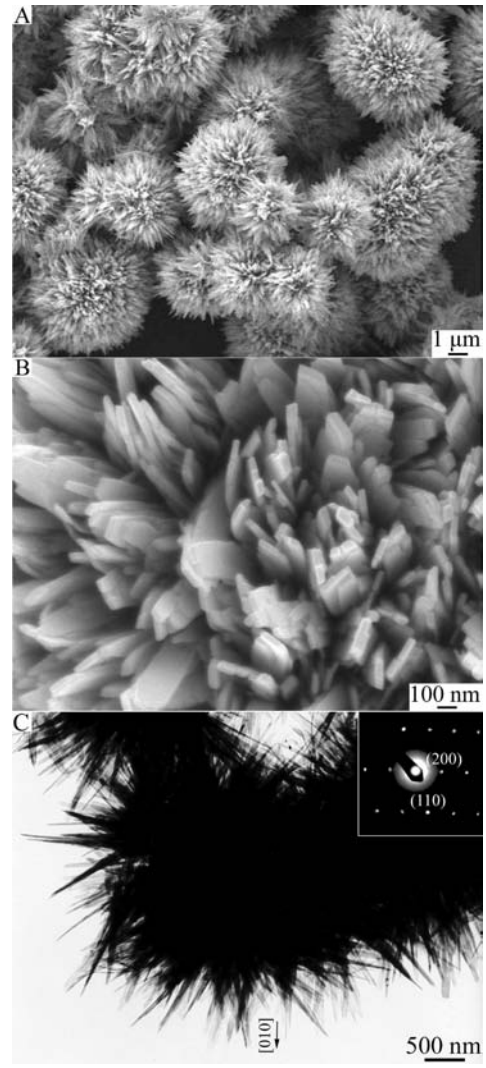

Figure 1. SEM and TEM images of urchin-like VO_2(B) nanostructures composed of radially aligned nanobelts synthesized with 0.05 mol/L oxalic acid at 180 °C for 12 h. (A) Low-magnification SEM image, (B) high-magnification SEM image, and (C) TEM image. The inset in part C shows a typical ED pattern taken from an individual nanobelt.

Characterization. The morphologies and sizes of the resulting products were characterized by field-emission scanning electron microscopy (FE-SEM, JSM 6700F) and transmission electron microscopy (TEM, JEM 2000EX). The crystal structures of the resulting products were characterized by powder X-ray diffraction (XRD, Rigaku D-max-γA XRD with Cu Kα radiation, $\gamma = 1.54178$ Å). UV−vis spectra of the resulting products were determined on Cary 500 UV−vis−NIR spectrophotometer.

Results and Discussion

Figure 1 presents typical SEM and TEM images of VO_2(B) nanostructures synthesized with 0.05 mol/L oxalic acid at 180 °C for 12 h. As shown in low-magnification SEM image (part A of Figure 1), one can observe that the resulting dark-blue products are a large amount of spherical VO_2(B) nanostructures with diameters of 2−6 μm, which are highly

(17) Manning, T. D.; Parkin, I. P.; Pemble, M. E.; Sheet, D.; Vernardou, D. *Chem. Mater.* **2004**, *16*, 744.
(18) Binions, R.; Hyett, G.; Piccirillo, C.; Parkin, I. P. *J. Mater. Chem.* **2007**, *17*, 4652.
(19) Rozen, J.; Lopez, R.; Haglund, R. F., Jr.; Feldman, L. C. *Appl. Phys. Lett.* **2006**, *88*, 081902.
(20) Balu, R.; Ashrit, P. V. *Appl. Phys. Lett.* **2008**, *92*, 021904.
(21) Lopez, R.; Boatner, L. A.; Haynes, T. E.; Feldman, L. C.; Haglund, R. F., Jr. *J. Appl. Phys.* **2002**, *92*, 4031.
(22) Peng, Z.; Jiang, W.; Liu, H. *J. Phys. Chem. C* **2007**, *111*, 1119.
(23) Liu, J.; Li, Q.; Wang, T.; Yu, D.; Li, Y. *Angew. Chem., Int. Ed.* **2004**, *43*, 5048.
(24) Li, G.; Chao, K.; Peng, H.; Chen, K.; Zhang, Z. *Inorg. Chem.* **2007**, *46*, 5787.
(25) Chen, X.; Wang, X.; Wang, Z.; Wan, J.; Liu, J.; Qian, Y. *Nanotechnology* **2004**, *15*, 1685.
(26) Armstrong, G.; Canales, J.; Armstrong, A. R.; Bruce, P. G. *J. Power Sources* **2008**, *178*, 723.
(27) Chen, W.; Peng, J.; Mai, L.; Yu, H.; Qi, Y. *Chem. Lett.* **2004**, *33*, 1366.
(28) Tsang, C.; Manthiram, A. *J. Electrochem. Soc.* **1997**, *144*, 520.
(29) Li, X.; Chen, X.; Chen, X.; Han, C.; Shi, C. *J. Cryst. Growth* **2007**, *309*, 43.
(30) Li, G.; Pang, S.; Wang, Z.; Peng, H.; Zhang, Z. *Eur. J. Inorg. Chem.* **2005**, 2060.
(31) Pang, S.; Li, G.; Zhang, Z. *Macromol. Rapid Commun.* **2005**, *26*, 1262.
(32) Li, G.; Pang, S.; Jiang, L.; Guo, Z.; Zhang, Z. *J. Phys. Chem. B* **2006**, *110*, 9383.
(33) Li, G.; Jiang, L.; Peng, H. *Mater. Lett.* **2007**, *61*, 4070.

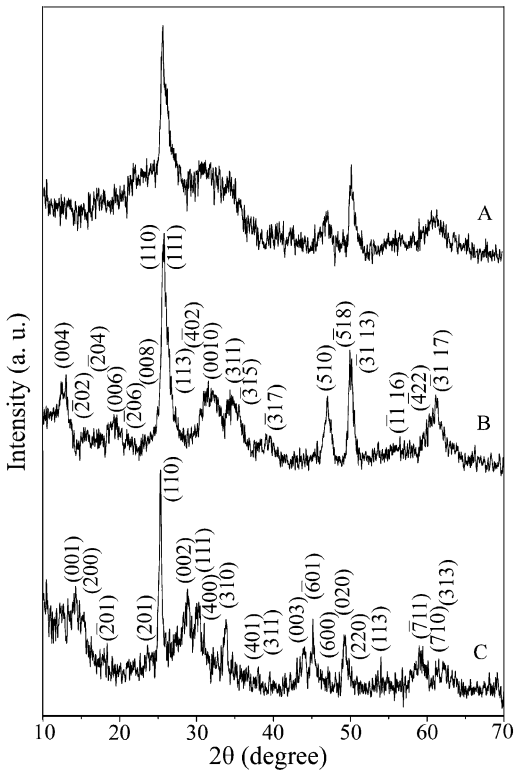

Figure 2. XRD patterns of the resulting products synthesized with 0.05 mol/L oxalic acid at 180 °C for different reaction times: (A) 0.5 h, (B) 2 h, and (C) 12 h.

reminiscent of urchin-like nanostructures. The urchin-like VO_2(B) nanostructures are composed of radially aligned nanorods. In a high-magnification SEM image in part B of Figure 1, it is clear that the geometrical shapes of VO_2(B) nanorods are belt with rectangular cross section. The thickness and width of VO_2(B) nanobelts are 20−30 nm and 50−150 nm, respectively. The ends of the nanobelts are irregular. The urchin-like VO_2(B) nanostructures can be further confirmed by the TEM image in part C of Figure 1. As shown in the inset in part C of Figure 1, the electron diffraction (ED) pattern taken from an individual nanobelt can be attributed to monoclinic VO_2(B), indicating that the nanobelts are structurally uniform and single crystalline with the growth direction along [010].

To investigate the formation process of the urchin-like VO_2(B) nanostructures composed of radially aligned nanobelts, time-dependent experiments are carried out at 180 °C for different reaction times. Parts A−C of Figure 2 show XRD patterns of the resulting products synthesized with 0.05 mol/L oxalic acid at 180 °C for 0.5, 2, and 12 h, respectively. After 0.5 h, the color of the solution changes from orange to green, indicating that V^{5+} ions in peroxovanadic acid are reduced partly to V^{4+} ions by oxalic acid. As shown in part A of Figure 2, the diffraction peaks of the resulting products can be indexed to monoclinic $V_{10}O_{24}\cdot 12H_2O$ with lattice contents $a = 11.7$ Å, $b = 3.63$ Å, $c = 29.06$ Å, and $\beta = 101.5°$, which is in agreement with literature values (JCPDS 251006). The water in the interlamellar region of $V_{10}O_{24}\cdot 12H_2O$ results in the large d_{004} spacing of 7.08 Å. After 2 h, monoclinic $V_{10}O_{24}\cdot 12H_2O$ can also be obtained. In comparison with part A of Figure 2, the intensity of the diffraction peaks increases, indicating that the products have higher crystallinity. After 12 h, the color of the solution changes from green to dark blue. As shown in part B of Figure 2, the diffraction peaks of the resulting products can be ascribed to monoclinic crystalline phase VO_2(B) with lattice contents $a = 12.1$ Å, $b = 3.70$ Å, $c = 6.43$ Å, and $\beta = 107.0°$ (JCPDS 812392), revealing that all of the V^{5+} ions in $V_{10}O_{24}\cdot 12H_2O$ have been further reduced to V^{4+} ions by oxalic acid in the reaction.

Representative SEM images of the resulting products synthesized with 0.05 mol/L oxalic acid at 180 °C for different reaction times are presented in Figure 3. When the reaction is performed for 0.5 h, as shown in part A of Figure 3, the products exhibit draped filmlike morphology. After 2 h, the low-magnification SEM image in part B of Figure 3 reveals that a large quantity of urchin-like $V_{10}O_{24}\cdot 12H_2O$ nanostructures with diameters of 2−3 μm are formed in the products. In the high-magnification SEM image (part C of Figure 3), it is found that the urchin-like $V_{10}O_{24}\cdot 12H_2O$ nanostructures are constituted by irregular nanobelts. The thickness, width, and length of the nanobelts are about 10−20 nm, 50−150 nm, and 1−2 μm, respectively. After 6 h, the diameters of the urchin-like nanostructures in part D of Figure 3 increase to 3−6 μm. The high-magnification SEM image in part E of Figure 3 shows that the urchin-like nanostructures consist of a lot of radially aligned nanobelts with thicknesses of 30−50 nm, and widths of 100−300 nm. In combination with Figure 1, the formation of urchin-like VO_2(B) nanostructures is related to a reduction−dehydration phase-transition process, which has never been observed in the literature. The thickness of VO_2(B) nanobelts is clearly smaller than that of $V_{10}O_{24}\cdot 12H_2O$ nanobelts, indicating the dehydration process for the formation of VO_2(B). However, after 24 h, on the basis of the vestiges in part F of Figure 3, it is clear that the urchin-like VO_2(B) nanostructures synthesized for 12 h are disassembled in situ into dissociated VO_2(B) nanobelts. A typical high-magnification SEM image of the dissociated VO_2(B) nanobelts (the inset in part F of Figure 3) shows that the thickness and width of VO_2(B) nanobelts are similar to those in Figure 1. The ends of VO_2(B) nanobelts are not very sharp.

UV−vis spectra of the resulting products synthesized with 0.05 mol/L oxalic acid at 180 °C for 0.5 and 2 h are shown in parts A and B of Figure 4, respectively. The bands around 260 and 390 nm can be related to charge transfer between oxygen and V^{5+} ions.[34] Their intensity decreases as the reaction time increases from 0.5 to 2 h. The weak band centered around 760 nm corresponds to the d−d electronic transition of V^{4+} ions,[34,35] indicating that V^{5+} ions in peroxovanadic acid are reduced partly to V^{4+} ions by oxalic acid.

The influences of the concentration of oxalic acid on the shapes of VO_2(B) nanostructures have been investigated. Figure 5 represents typical SEM images of VO_2(B) nano-

(34) Gharbi, N.; Sanchez, C.; Livage, J.; Lemerle, J.; Néjem, L.; Lefebvre, J. *Inorg. Chem.* **1982**, *21*, 2758.
(35) Takahashi, K.; Limmer, S. J.; Wang, Y.; Cao, G. *J. Phys. Chem. B* **2004**, *108*, 9795.

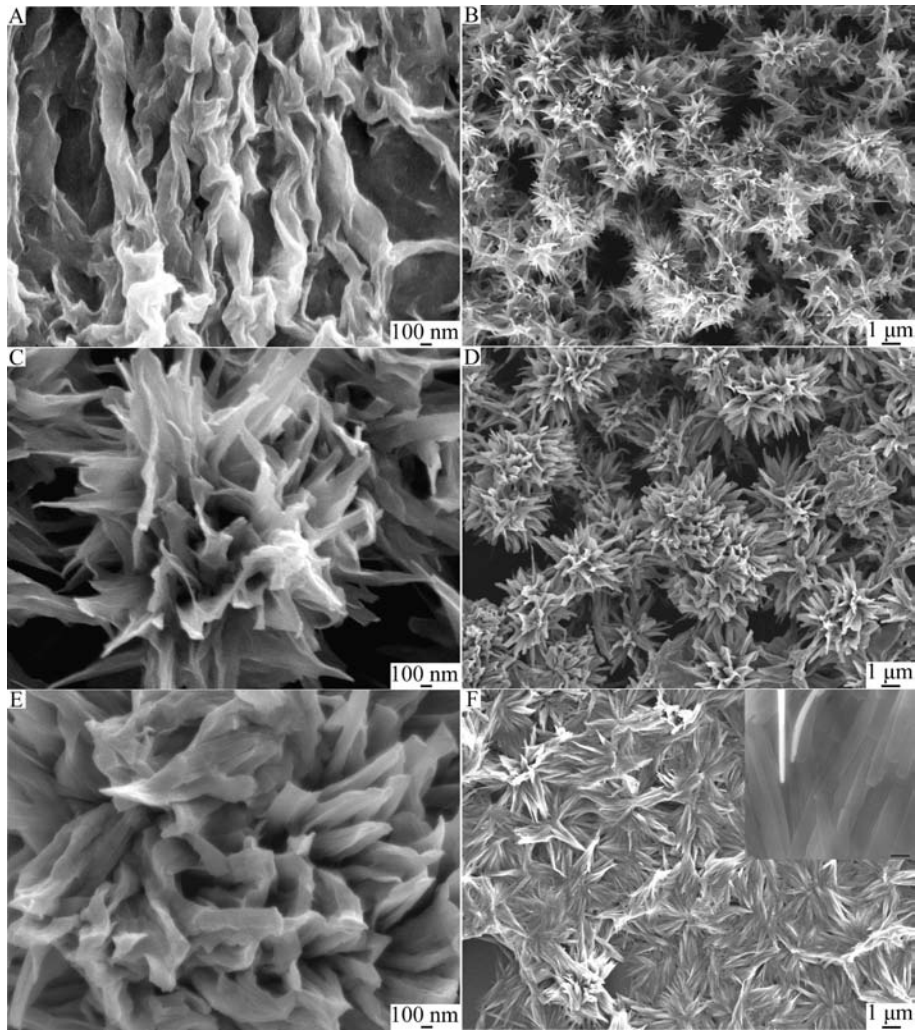

Figure 3. SEM images of the resulting products synthesized with 0.05 mol/L oxalic acid at 180 °C for different reaction times: (A) 0.5 h, (B, C) 2 h, (D, E) 6 h, and (F) 24 h. The inset in part F of Figure 3 shows a typical high-magnification SEM image, and the scale bar is 100 nm.

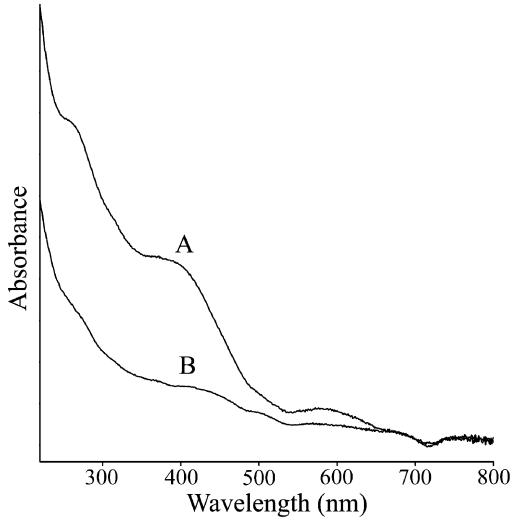

Figure 4. UV−vis spectra of the resulting products synthesized with 0.05 mol/L oxalic acid at 180 °C for different reaction times: (A) 0.5 h and (B) 2 h.

structures synthesized with different concentrations of oxalic acid at 180 °C for 24 h. When the concentration of oxalic acid decreases to 0.02 mol/L, VO_2(B) nanobelts with two sharp ends and lengths of up to several micrometers (part A of Figure 5) are obtained. The width of VO_2(B) nanobelts decreases gradually from the middle part (60−150 nm) to the ends to form needle-like tips. Whereas, as the concentration of oxalic acid increases to 0.08 mol/L, VO_2(B) aggregates composed of nanoparticles, nanobelts, and nanosheets are formed in the products (part B of Figure 5), which is very different from our previous results without the aid of H_2O_2.[24] The thickness and widths of the nanobelts are larger than those in part F of Figure 3 and part A of Figure 5.

The solution-based synthesis is dependent on the reaction between peroxovanadic acid and oxalic acid. The basic reactions can be described as follows:

$$V_2O_5 + 4H_2O_2 \rightarrow 2[VO(O_2)_2]^- + 2H^+ + 3H_2O \quad (1)$$

$$10[VO(O_2)_2]^- + 10H^+ + C_2H_2O_4 + 6H_2O \rightarrow V_{10}O_{24}\cdot 12H_2O + 2CO_2 + 10O_2 \quad (2)$$

$$V_{10}O_{24}\cdot 12H_2O + 4C_2H_2O_4 \rightarrow 10\ VO_2(B) + 8CO_2 + 16H_2O \quad (3)$$

The formation of VO_2(B) nanostructures undergoes a reduction−dehydration phase-transition and disassembly process. Before the reduction reaction, V_2O_5 dissolves in H_2O_2 aqueous solution to form an orange solution of diperoxo

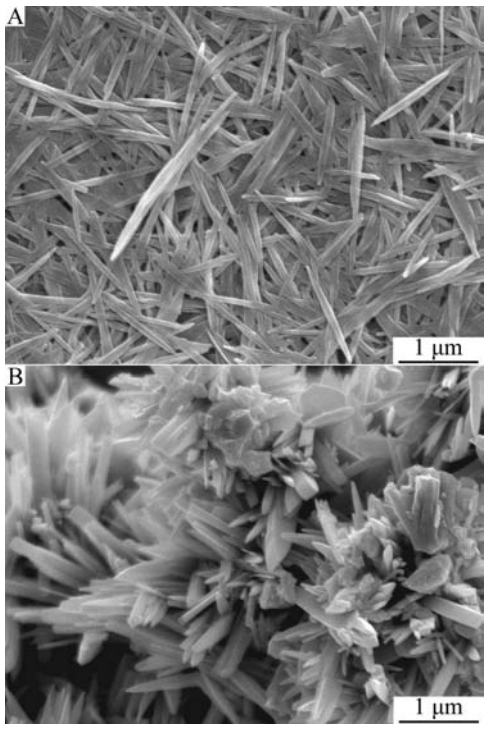

Figure 5. SEM images of the resulting products synthesized with different concentration of oxalic acid at 180 °C for 24 h: (A) 0.02 mol/L and (B) 0.08 mol/L.

anions $[VO(O_2)_2]^-$ (eq 1).[36,37] At the early stage of the hydrothermal reaction, the solution of diperoxo anions can be reduced partly by oxalic acid to form $V_{10}O_{24}\cdot 12H_2O$ clusters (eq 2), which is different from that synthesized with other vanadium precursors.[23−29] Then the newly formed $V_{10}O_{24}\cdot 12H_2O$ clusters can serve as the sites of heterogeneous nucleation for the formation of urchin-like $V_{10}O_{24}\cdot 12H_2O$ nanostructures composed of nanobelts due to its layered crystal structures in nature. Then the newly formed $V_{10}O_{24}\cdot 12H_2O$ clusters can serve as the sites of heterogeneous nucleation for the formation of urchin-like $V_{10}O_{24}\cdot 12H_2O$ nanostructures composed of nanobelts due to its layered crystal structures in nature. With the reduction reaction proceeding, $V_{10}O_{24}\cdot 12H_2O$ nanostructures are transformed in situ into urchin-like VO_2(B) nanostructures composed of radially aligned nanobelts by a reduction−dehydration process (eq 3). This formation of urchin-like VO_2(B) nanostructure can be ascribed to a topotactic transformation process from urchin-like $V_{10}O_{24}\cdot 12H_2O$ nanostructures. As reported in literature, water molecules in the interlamellar region of $V_2O_5\cdot nH_2O$ are removed gradually with the reaction time increased,[32] whereas V^{5+} ions in $V_{10}O_{24}\cdot 12H_2O$ can be reduced further to V^{4+} ions by oxalic acid. The in situ reduction−dehydration reaction between $V_{10}O_{24}\cdot 12H_2O$ and oxalic acid results in the formation of urchin-like VO_2(B) nanostructure. As the reaction time is prolonged, the urchin-like VO_2(B) nanostructures can be disassembled into discrete nanobelts possibly due to the stress−strain of the phase-transition process in the center part.

Conclusions

In summary, we have developed a facile homogeneous reduction reaction between peroxovanadic acid and oxalic acid to synthesize urchin-like VO_2(B) nanostructures composed of radially aligned nanobelts. The urchin-like VO_2(B) nanostructures are formed in situ by a phase transition from monoclinic $V_{10}O_{24}\cdot 12H_2O$ to monoclinic VO_2(B) during the reduction−dehydration process, which are disassembled into dissociated VO_2(B) nanobelts with the reaction time increased. The shapes of VO_2(B) nanobelts can be controlled by adjusting the concentration of oxalic acid.

Acknowledgment. We gratefully acknowledge financial support from the National Natural Science Foundation of China (NSFC 50702028) and Shandong Distinguished Middle-aged and Young Scientist Encourage and Reward Foundation (2007BS04008).

IC801620N

(36) Alonso, B.; Livage, J. *J. Solid State Chem.* **1999**, *148*, 16.
(37) Fontenot, C. J.; Wiench, J. W.; Pruski, M.; Schrader, G. L. *J. Phys. Chem. B* **2000**, *104*, 11622.